Preparation and redox properties of fluorinated 1,3-diphenylisobenzofurans

Jiří Kaleta, Ludmila Šimková, Alan Liška, Daniel Bím, Jenica M.L. Madridejos, Radek Pohl, Lubomír Rulíšek, Josef Michl, Jiří Ludvík

PII: S0013-4686(19)31527-0

DOI: https://doi.org/10.1016/j.electacta.2019.134659

Reference: EA 134659

To appear in: *Electrochimica Acta*

Received Date: 13 June 2019

Revised Date: 1 August 2019

Accepted Date: 8 August 2019

Please cite this article as: Jiří. Kaleta, L. Šimková, A. Liška, D. Bím, J.M.L. Madridejos, R. Pohl, Lubomí. Rulíšek, J. Michl, Jiří. Ludvík, Preparation and redox properties of fluorinated 1,3-diphenylisobenzofurans, *Electrochimica Acta* (2019), doi: https://doi.org/10.1016/j.electacta.2019.134659.

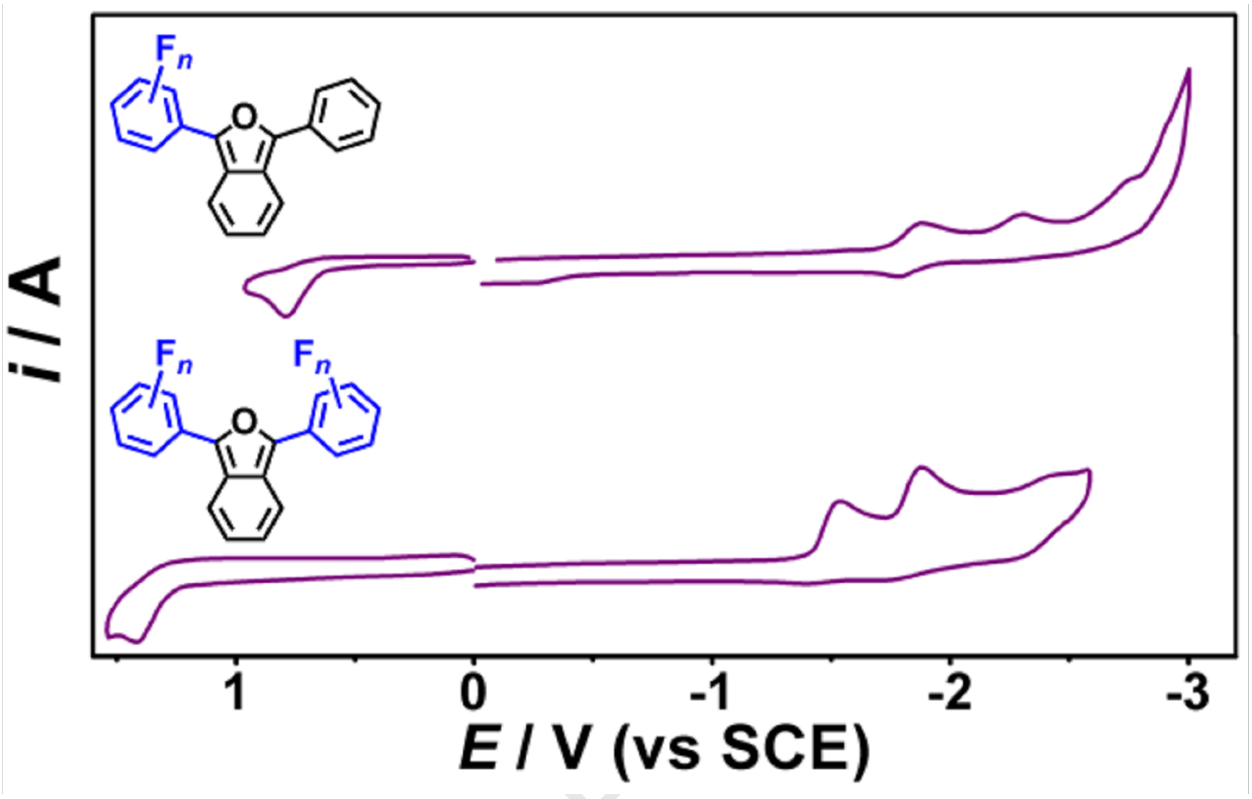

Preparation and Redox Properties of Fluorinated 1,3-Diphenylisobenzofurans

Jiří Kaleta [a,b], Ludmila Šimková [c], Alan Liška [c], Daniel Bím [a,c], Jenica M. L. Madridejos [a], Radek Pohl [a], Lubomír Rulíšek [a], Josef Michl [a,b] and Jiří Ludvík [c]*

[a] *Institute of Organic Chemistry and Biochemistry, Czech Academy of Sciences, Flemingovo nám. 2, 16610 Prague 6, Czech Republic, jiri.kaleta@uochb.cas.cz*

[b] *Department of Chemistry and Biochemistry, University of Colorado, Boulder, CO 80309-0215, United States, josef.michl@colorado.edu*

[c] *J. Heyrovský Institute of Physical Chemistry, Czech Academy of Sciences, Dolejškova 2155/3, 182 23 Prague 8, Czech Republic. jiri.ludvik@jh-inst.cas.cz ;* *corresponding author

ABSTRACT

Eleven fluorinated 1,3-diphenylisobenzofurans, materials that are promising to perform efficient singlet fission, have been synthesized and their electrochemical reduction and oxidation in non-aqueous dimethylformamide examined. The redox properties are not changed continuously with increasing number of fluorine substituents but there are some qualitative turns in behavior for specific types of substitution revealing a discontinuity requiring deeper investigation. The DFT calculations confirm the trends observed experimentally by correlation of experimental and calculated data. The differences between the geometries of the neutral species and their radical ions were computed and rationalized.

KEYWORDS

Fluorinated 1,3-Diphenylisobenzofurans; singlet fission; synthesis; oxidation/reduction; DFT calculations.

1 INTRODUCTION

1,3-Diphenylisobenzofuran (**1**) is one of the few materials that are known to perform highly efficient singlet fission,[1,2] a photophysical process in which a singlet exciton is converted into two triplet excitons. Singlet fission has attracted increasing attention because it promises[3] to increase the maximum theoretical efficiency of inexpensive single-junction solar cells beyond the Shockley-Queisser limit[4] of 1/3. So far, it has not found its way into practice because none of the materials in which it proceeds efficiently are sufficiently sturdy. This is certainly true of **1**, which is very

sensitive to a combination of light and air. Quantum theory has been quite helpful in efforts to guide the search for more efficient materials for singlet fission use, both when it comes to the choice of chromophores and when it comes to their mode of packing.

The most important criterion in the selection of chromophores, $E(S_1) \geq 2\ E(T_1)$, assures that the singlet fission process is isoergic or even better, somewhat exoergic. This criterion is rarely fulfilled. A class of compounds that are likely to meet the requirement are biradicaloids, species formally derived from perfect biradicals by sufficient but not excessive covalent perturbation.[5] This was the consideration that led to the original choice of **1** as a molecule suitable for singlet fission.[6]

The critical importance of molecular packing was underscored upon closer examination of **1**. This material exists in two crystalline forms. While one of them performs singlet fission very efficiently, the other performs it hardly at all.[7] General theoretical guidance toward optimization of crystal packing has been formulated,[8,9,10] but is still in early stages.

One way to test the theoretical notions concerning crystal packing that is optimal for singlet fission would be to study singlet fission on additional chromophores[11,12] that crystallize in two or more crystal forms. We have decided to try another approach and to take advantage of the fact that certain substituents have little effect on electronic excitation energies and presumably other properties relevant to singlet fission, yet are capable of modifying crystal packing dramatically. This should provide relatively easy access to a larger pool of data. Starting with **1**, we have examined the effect of alkylation, but found that it tends to produce amorphous materials.[13] In order to investigate the effect of fluorination, which also does not modify the electronic spectra of aromatics much but tends to affect crystal packing strongly,[14,15,16] we needed to gain access to a fair number of fluorinated derivatives of **1**, few of which are known.

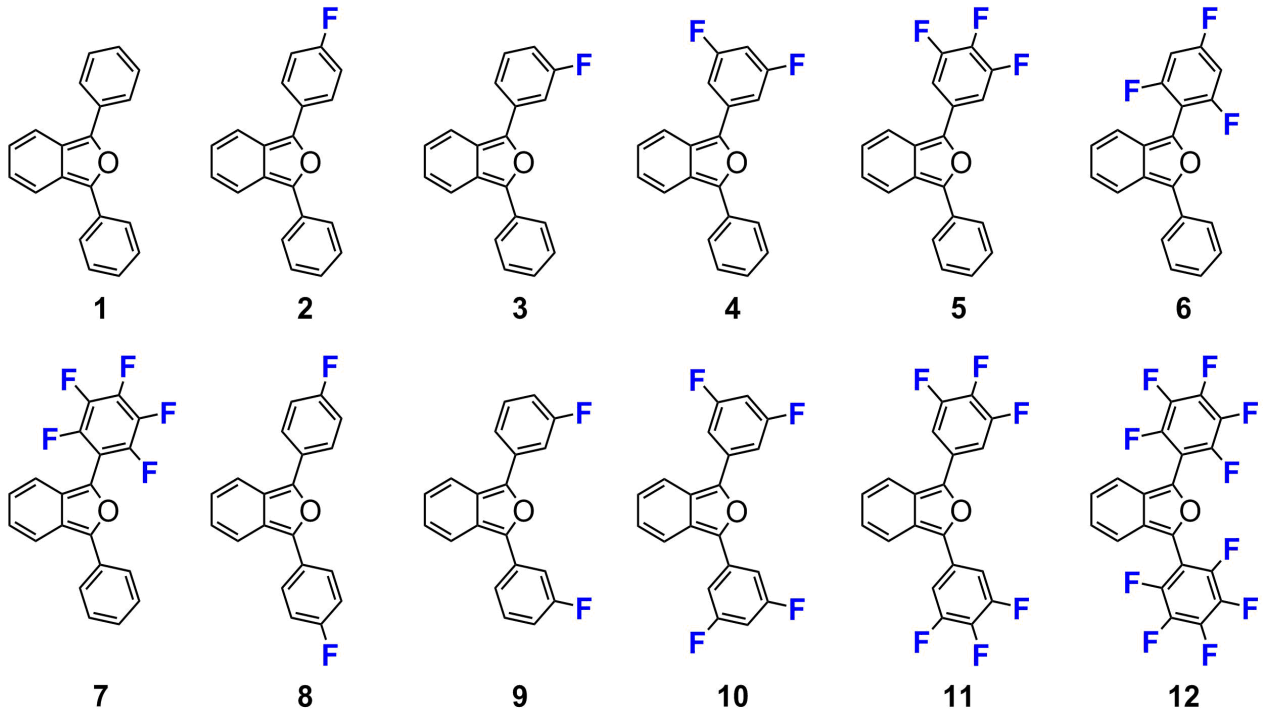

Figure 1. Structures of **1** and its partially fluorinated derivatives **2 - 12**.

Presently, we report the preparation and characterization of eleven new compounds of this type (Figure 1). Since redox properties of the chromophores play a significant role in understanding singlet fission due to the usually dominant mechanistic importance of virtual charge-separated states in the process, we have primarily examined their electrochemical reduction and oxidation using various electrode materials in non-aqueous DMF, with focus on the potentials of the first uptake and loss of an electron. The experimental data were compared with those of density functional theory (DFT) calculations. Besides the redox characterization, the other task for the electrochemical treatment of these polyfluorinated derivatives was to solve the question, whether the redox properties are changed continuously with increasing number of fluorine substituents or if there are some qualitative turns in behavior for specific types of substitution which would reveal a discontinuity relevant to the desired properties and requiring deeper investigation.

2 EXPERIMENTAL

2.1 Electrochemistry

DC-polarography and cyclic voltammetry were carried out in *N*,*N*-dimethylformamide (DMF, purified and dried by double distillation[17]) containing 0.1 M tetrabutylammonium

hexafluorophosphate ($TBAPF_6$) as the supporting electrolyte and 1×10^{-3} M solutions of **1** - **12** deoxygenated with argon. A dropping mercury electrode (DME) with a controlled drop time (1 s) was used in DC-polarography. A platinum, glassy carbon disk (GC, area ca. 1 mm^2), boron doped diamond (BDDE) stationary electrode, or a hanging mercury drop electrode (HMDE) were used for cyclic voltammetry, measured at four different scan rates (50, 100, 200 and 500 $mV.s^{-1}$). The reduction potentials obtained at the four different electrodes differed by less than the experimental error (±10 mV). The oxidation peaks were broader and their positions again agreed within the experimental uncertainty of ±20 mV on three of the electrodes. The values obtained with the GC electrode were systematically less positive by about 30 mV and are presumably the closest to the thermodynamic values.

The auxiliary electrode was made of a platinum wire and a saturated calomel electrode (SCE) separated from aprotic solution by a salt bridge served as the reference electrode. All experiments were carried out in an undivided 10 mL cell and were conducted by the analog potentiostat PA4 with an XY recorder, both Laboratorní přístroje Praha and by the computer driven digital potentiostat PGSTAT101 (Autolab-Metrohm) using software NOVA.

2.2 **Calculations**

Standard density functional theory calculations were performed using the Turbomole 7.1 program.[18] First, all structures were optimized at the RI-BP86-D3/def-TZVP level of theory[19,20,21,22,23] using implicit solvation conductor-like screening model (COSMO)[24] with ε_r= 37.5, corresponding to the dielectric constant of DMF. After each geometry optimization, single-point calculations using RI-B3LYP-D3/def2-TZVPD[25,26] and RI-PBE-D3/def2-TZVPD[27] methods were carried out to obtain in vacuo E_{el} energies as defined in Equation 2. The solvation free energy difference $G_{solv}(T)$ was calculated using the conductor-like screening model for real solvents (COSMO-RS) with the radii-based isosurface cavity ($cosmo_isorad keyword) and the COSMOtherm parameter set BP_TZVPD_FINE_C30_1701.ctd as available in COSMOtherm17.[28] The COSMO-RS calculations were carried out following the recommended protocol: the RI-BP86-D3/def2-TZVPD/COSMO($\varepsilon_r = \infty$) ≡ $E_{COSMO,\infty}$ and RI-BP86-D3/def2-TZVPD/in vacuo ≡ $E_{in\ vacuo}$ single-point calculations (on top of geometry optimizations with COSMO) are used to calculate $G_{solv}(T) = (E_{COSMO,\infty} - E_{in\ vacuo}) + \mu_{COSMO\text{-}RS}(T)$, where $\mu(T)$ is the temperature-dependent COSMO-RS chemical potential.[29] The last term in Equation 2, $\Delta(E_{ZPVE} + pV - RT \ln Q)$, was obtained from frequency calculations with the rigid-rotor/harmonic-oscillator approximation (for p = 1 bar), considering low-frequency vibration modes (≤100 cm^{-1}) to contribute to Q as hindered rotors.[30] For frequency calculations, the gas-phase optimized structures at RI-BP86-D3/def-TZVP level of

theory were used.

Molecular orbitals were calculated at the RI-B3LYP-D3/def2-TZVPD level of theory.

2.3 X-ray Diffraction

Crystallographic data for **21** were collected on Bruker D8 VENTURE Kappa Duo PHOTON100 by IμS micro-focus sealed tube with CuKα radiation (λ = 1.54178 Å) at 150(2) K. The structures were solved by direct methods (XT)[31] and refined by full matrix least squares based on F^2 (SHELXL2014).[32] The hydrogen atoms on carbon atoms were fixed into idealized positions (riding model) and assigned temperature factors of $H_{iso}(H) = 1.2\ U_{eq}$(pivot atom).

2.4 Materials

All reactions were carried out under argon atmosphere with dry solvents freshly distilled under anhydrous conditions, unless otherwise noted. Standard Schlenk and vacuum line techniques were employed for all manipulations of air- or moisture-sensitive compounds. Yields refer to isolated, chromatographically and spectroscopically homogenous materials, unless otherwise stated.

THF and ether were dried over sodium with benzophenone and distilled under argon prior to use. All other reagents were used as supplied unless otherwise stated.

2.5 Procedures

Analytical thin-layer chromatography (TLC) was performed using precoated TLC aluminum sheets (Silica gel 60 F_{254}). TLC spots were visualized using either UV light (254 nm) or a 5% solution of phosphomolybdic acid in ethanol, and heat (200 °C) as a developing agent. Flash chromatography was performed using silica gel (high purity grade, pore size 60 Å, 70 - 230 mesh). Melting points are reported uncorrected. Infrared spectra (IR) were recorded in KBr pellets. Chemical shifts in ^{1}H, and ^{13}C spectra are reported in ppm on the δ scale relative to $CHCl_3$ (δ = 7.26 ppm for ^{1}H NMR), and $CHCl_3$ (δ = 77.0 ppm for ^{13}C NMR) as internal references. Splitting patterns are assigned s = singlet, d = doublet, t = triplet, m = multiplet, br = broad signal.

2.6 Syntheses

1-(4-Fluorophenyl)-3-phenylisobenzofuran (**2**). A previously published procedure[14] was adapted as follows: An argon filled 50 mL two-necked flask equipped with stir bar and a gas condenser was charged with magnesium turnings (535 mg, 22.000 mmol). After three successive vacuum/argon cycles, ether (40 mL) and one grain of iodine were added, and a brownish suspension was stirred for 15 min at room temperature. Subsequently 1-bromo-4-fluorobenzene (2.35 mL, 21.404 mmol) was added dropwise. An exothermic reaction was followed by changes of

the color of the reaction mixture from original brown, through colorless to final grayish. This suspension was stirred 120 min at room temperature and then 3-phenylisobenzofuran-1(3*H*)-one (**19**) (3.000 g, 14.269 mmol) was added and stirring was continued for 16 h. A dense grayish solid precipitated. Subsequently trifluoroacetic acid (2 mL) was added dropwise and the reaction mixture was stirred for additional 15 min. The black reaction mixture was diluted with ether (50 mL), washed with a saturated aqueous solution of $NaHCO_3$ (3 × 30 mL), and dried over $MgSO_4$. Solvent was removed under reduced pressured and column chromatography on silica gel (hexane/ethyl acetate - 4:1) gave **2** as an yellow crystalline solid (1.260 g, 4.370 mmol, 31%).

Mp 113.5 - 114.2 °C. ^{1}H NMR (500 MHz, $CDCl_3$): δ 6.99 - 7.04 (m, 2H), 7.17 - 7.20 (m, 2H), 7.29 - 7.32 (m, 1H), 7.48 - 7.51 (m, 2H), 7.76 (m, 1H), 7.83 (m, 1H), 7.90 (m, 2H), 7.93 (m, 2H). ^{13}C {^{1}H} NMR (125 MHz, $CDCl_3$): δ 116.0 (d, $J_{C,F}$ = 21.9 Hz), 119.8, 120.2, 121.7 (d, $J_{C,F}$ = 1.3 Hz), 122.0, 124.7, 125.1, 125.2, 126.4 (d, $J_{C,F}$ = 7.9 Hz), 126.9, 128.0 (d, $J_{C,F}$ = 3.4 Hz), 128.9, 131.5, 142.9 (d, $J_{C,F}$ = 1.2 Hz), 143.7 (d, $J_{C,F}$ = 1.9 Hz), 161.7 (d, $J_{C,F}$ = 247.7 Hz). ^{19}F NMR (470 MHz, $CDCl_3$): δ -110.73 (tt, $^{1}J_{F,H}$ = 8.6 Hz, $^{2}J_{F,H}$ = 5.4 Hz, 1F). IR (KBr): 3053, 1662, 1627, 1597, 1573, 1547, 1511, 1490, 1464, 1447, 1438, 1404, 1367, 1296, 1282, 1225, 1203, 1153, 1130, 1095, 1071, 1028, 1013, 993, 980, 937, 908, 833, 813, 765, 750, 742, 721, 711, 691, 659, 642, 632, 617, 608, 575, 552, 511, 487 cm^{-1}. MS, *m/z* (%): 288.1 (100, M), 270.1 (6), 259.1 (43), 239.1 (12), 183.1 (12), 165.1 (14), 144.0 (13), 95.0 (16), 77.0 (9). HRMS, (EI) for ($C_{20}H_{13}FO^{+}$): calcd 288.0950, found 288.0947. Anal. Calcd. for $C_{20}H_{13}FO$: C, 83.32; H, 4.54. Found: C, 83.13; H, 4.65.

General Procedure for Synthesis of Asymmetric Fluorinated DPIBF Derivatives (GP1). An argon filled 50 mL two-necked flask equipped with a stir bar and a gas condenser was charged with magnesium turnings (129 mg, 5.300 mmol). After three successive vacuum/argon cycles, THF (15 mL) and one grain of iodine were added, and the brownish suspension was stirred for 15 min at room temperature. Subsequently fluorinated bromobenzene (5.200 mmol) was added. An exothermic reaction was followed by changes of the color of the reaction mixture from original brown, through colorless to final grayish. This suspension was stirred 2 h at room temperature and then 3-phenylisobenzofuran-1(3*H*)-one (**19**) (1.000 g, 4.757 mmol) was added and stirring continued for 16 h. Then Ac_2O (4 mL) was added dropwise and the reaction mixture was refluxed at the temperature of the oil bath 70 °C for additional 30 min. A dense yellowish precipitate was formed. The yellow suspension was cooled to room temperature, diluted with ether (100 mL), and washed with a saturated aqueous solution of $NaHCO_3$ (3 × 15 mL). The deep yellow organic phase was dried over $MgSO_4$. Solvents were removed under reduced pressure and column chromatography on silica gel (hexane/ethyl-acetate - 4:1) afforded products as yellow crystalline

solids.

1-(3-Fluorophenyl)-3-phenylisobenzofuran (**3**) was synthesized from 1-bromo-3-fluorobenzene (**14**) (581 μL, 5.200 mmol), magnesium (129 mg, 5.300 mmol), and **19** (1.000 g, 4.757 mmol) in THF (15 mL) according to **GP1**. Compound **3** was obtained as a bright yellow crystalline solid (1.216 g, 4.218 mmol, 89%).

Mp 130.9 - 132.0 °C. ^{1}H NMR (400 MHz, $CDCl_3$): δ 6.94 - 7.01 (m, 1H), 7.01 - 7.10 (m, 2H), 7.29 - 7.35 (m, 1H), 7.40 - 7.47 (m, 1H), 7.47 - 7.53 (m, 2H), 7.60 - 7.65 (m, 1H), 7.71 - 7.74 (m, 1H), 7.80 - 7.87 (m, 2H), 7.93 - 7.97 (m, 2H). ^{13}C {^{1}H} NMR (125 MHz, $CDCl_3$): δ 111.3 (d, $J_{C,F}$ = 23.6 Hz), 113.5 (d, $J_{C,F}$ = 21.5 Hz), 119.8, 120.2 (d, $J_{C,F}$ = 2.8 Hz), 120.3, 122.1, 122.7, 125.0, 125.2, 125.8, 127.2, 129.0, 130.5 (d, $J_{C,F}$ = 8.6 Hz), 131.3, 133.5 (d, $J_{C,F}$ = 8.6 Hz), 142.3 (d, $J_{C,F}$ = 3.2 Hz), 144.4, 163.3 (d, $J_{C,F}$ = 245.1 Hz). ^{19}F NMR (470 MHz, $CDCl_3$): δ -108.92 (ddd, $^{1}J_{F,H}$ = 10.3 Hz, $^{2}J_{F,H}$ = 8.6 Hz, $^{3}J_{F,H}$ = 6.0 Hz, 1F). IR (KBr): 3051, 3039, 1625, 1608, 1579, 1543, 1518, 1503, 1491, 1458, 1451, 1443, 1414, 1397, 1315, 1274, 1259, 1213, 1194, 1160, 1141, 1111, 1096, 1067, 1028, 1007, 994, 963, 951, 902, 877, 860, 854, 838, 829, 773, 762, 747, 744, 736, 723, 678, 665, 659, 599, 554, 523, 490 cm^{-1}. MS, *m/z* (%): 288.1 (100, M), 270.1 (5), 259.1 (23), 239.1 (11), 183.1 (10), 165.1 (9), 144.0 (10). HRMS, (EI) for ($C_{20}H_{13}FO^{+}$): calcd 288.0950, found 288.0948. Anal. Calcd. for $C_{20}H_{13}FO$: C, 83.32; H, 4.54. Found: C, 83.01; H, 4.45.

1-(3,5-Difluorophenyl)-3-phenylisobenzofuran (**4**) was synthesized from 1-bromo-3,5-difluorobenzene (**15**) (599 μL, 5.200 mmol), magnesium (129 mg, 5.300 mmol), and **19** (1.000 g, 4.757 mmol) in THF (15 mL) according to **GP1**. Compound **4** was obtained as a bright yellow crystalline solid (1.033 g, 2.867 mmol, 60%).

Mp 118.2 - 119.5 °C. ^{1}H NMR (400 MHz, $CDCl_3$): δ 6.67 - 6.73 (m, 1H), 7.02 - 7.11 (m, 2H), 7.32 - 7.44 (m, 3H), 7.48 - 7.53 (m, 2H), 7.73 - 7.76 (m, 1H), 7.82 - 7.86 (m, 1H), 7.91 - 7.94 (m, 2H). ^{13}C {^{1}H} NMR (125 MHz, $CDCl_3$): δ 101.7 (t, $J_{C,F}$ = 25.8 Hz), 106.9, 119.4, 120.5, 122.2, 123.3, 125.1, 125.3, 126.3, 127.6, 129.0, 131.0, 134.1 (t, $J_{C,F}$ = 10.7 Hz), 141.2 (d, $J_{C,F}$ = 3.6 Hz), 145.0, 163.5 (dd, $^{1}J_{C,F}$ = 247.2 Hz, $^{2}J_{C,F}$ = 13.5 Hz). ^{19}F NMR (470 MHz, $CDCl_3$): δ -105.76 (m, 2F). IR (KBr): 3081, 3025, 1621, 1589, 1547, 1504, 1483, 1453, 1443, 1403, 1327, 1280, 1221, 1195, 1184, 1142, 1115, 1073, 1004, 986, 952, 903, 852, 840, 835, 821, 760, 744, 734, 704, 685, 671, 618, 599, 532, 511, 504 cm^{-1}. MS, *m/z* (%): 306.1 (100), 277.1 (21), 257.1 (12), 229.0 (10), 201.1 (11), 165.1 (10), 153.0 (9). HRMS, (EI) for ($C_{20}H_{12}F_2O^{+}$): calcd 306.0856, found 306.0854. Anal. Calcd. for $C_{20}H_{12}F_2O$: C, 78.42; H, 3.95. Found: C, 78.12; H, 3.86.

1-Phenyl-3-(3,4,5-trifluorophenyl)isobenzofuran (**5**) was synthesized from 5-bromo-1,2,3-trifluorobenzene (**16**) (621 μL, 5.200 mmol), magnesium (129 mg, 5.300 mmol), and **19**

(1.000 g, 4.757 mmol) in THF (15 mL) according to **GP1**. Compound **5** was obtained as a bright yellow crystalline solid (1.078 g, 3.324 mmol, 70%).

Mp 129.5 - 131.0 °C. ^{1}H NMR (400 MHz, $CDCl_3$): δ 7.02 - 7.12 (m, 2H), 7.32 - 7.37 (m, 1H), 7.45 - 7.53 (m, 4H), 7.68 - 7.71 (m, 1H), 7.82 - 7.86 (m, 1H), 7.89 - 7.93 (m, 2H). ^{13}C {^{1}H} NMR (125 MHz, $CDCl_3$): δ 108.2 (m), 119.1, 120.5, 122.2, 122.9 (d, $J_{C,F}$ = 1.3 Hz), 125.1, 125.4, 126.5, 127.5 (td, $^{1}J_{C,F}$ = 9.1 Hz, $^{2}J_{C,F}$ = 4.7 Hz), 127.6, 129.1, 131.0, 138.4 (dt, $^{1}J_{C,F}$ = 252.5 Hz, $^{2}J_{C,F}$ = 15.6 Hz), 140.3 (d, $J_{C,F}$ = 2.8 Hz), 145.1, 151.8 (ddd, $^{1}J_{C,F}$ = 249.9 Hz, $^{2}J_{C,F}$ = 10.4 Hz, $^{3}J_{C,F}$ = 4.5 Hz). ^{19}F NMR (470 MHz, $CDCl_3$): δ -158.89 (tt, $J_{F,F}$ = 20.4 Hz, $J_{F,H}$ = 6.4 Hz, 1F); -130.19 (dd, $J_{F,F}$ = 20.4 Hz, $J_{F,H}$ = 8.7 Hz, 2F). IR (KBr): 3092, 3055, 1630, 1615, 1590, 1551, 1524, 1500, 1451, 1440, 1434, 1412, 1382, 1338, 1309, 1291, 1282, 1255, 1227, 1211, 1198, 1184, 1100, 1073, 1044, 1035, 1014, 951, 903, 866, 859, 855, 844, 833, 822, 762, 743, 699, 687, 664, 656, 611, 590, 563, 556, 508 cm^{-1}. MS, *m/z* (%): 324.1 (100, M), 306.1 (5), 295.1 (20), 275.1 (13), 247.0 (5), 162.0 (8). HRMS, (EI) for ($C_{20}H_{11}F_3O^{+}$): calcd 324.0762, found 324.0765. Anal. Calcd. for $C_{20}H_{11}F_3O$: C, 74.07; H, 3.42. Found: C, 73.83; H, 3.34.

1-Phenyl-3-(2,4,6-trifluorophenyl)isobenzofuran (**6**). An argon filled 50 mL two-necked flask equipped with stir bar and a gas condenser was charged with magnesium turnings (535 mg, 22.000 mmol). After three successive vacuum/argon cycles, ether (40 mL) and one grain of iodine were added, and the brownish suspension was stirred for 15 min at room temperature. Subsequently 1-bromo-2,4,6-trifluorobenzene (2.52 mL, 21.404 mmol) was added dropwise. The reaction mixture was stirred for 16 h at room temperature. Then 3-phenylisobenzofuran-1(3*H*)-one (**19**) (3.000 g, 14.269 mmol) was added and stirring continued for 5 h. A brownish oily phase was formed. Subsequently trifluoroacetic acid (2 mL) was added dropwise and the reaction mixture was stirred for additional 15 min. The black reaction mixture was diluted with ether (50 mL), washed with a saturated aqueous solution of $NaHCO_3$ (3 × 30 mL), and dried over $MgSO_4$. Solvent was removed under reduced pressured and column chromatography on silica gel (hexane/ethyl acetate - 4:1) provided **6** as an yellow crystalline solid (460 mg, 1.418 mmol, 10%).

Mp 112.0 - 113.1 °C. ^{1}H NMR (500 MHz, $CDCl_3$): δ 6.84 - 6.87 (m, 2H), 7.02 - 7.06 (m, 2H), 7.31 - 7.34 (m, 1H), 7.41 - 7.44 (m, 1H), 7.48 - 7.51 (m, 2H), 7.85 - 7.87 (m, 1H), 7.94 - 7.95 (m, 2H). ^{13}C {^{1}H} NMR (125 MHz, $CDCl_3$): δ 101.0 (m), 106.0 (td, $^{1}J_{C,F}$ = 18.7 Hz, $^{2}J_{C,F}$ = 5.1 Hz), 119.8 (t, $J_{C,F}$ = 4.2 Hz), 119.9, 121.1, 125.00, 125.04, 125.1, 125.27, 127.31, 128.9, 131.4, 132.3, 146.2, 160.0 (ddd, $^{1}J_{C,F}$ = 253.9 Hz, $^{2}J_{C,F}$ = 14.8 Hz, $^{3}J_{C,F}$ = 9.5 Hz), 162.5 (dt, $^{1}J_{C,F}$ = 251.8 Hz, $^{2}J_{C,F}$ = 15.4 Hz). ^{19}F NMR (470 MHz, $CDCl_3$): δ -103.81 (m, 2F), -103.76 (m, 1F). IR (KBr): 3091, 3057, 1639, 1595, 1577, 1508, 1495, 1451, 1442, 1400, 1352, 1266, 1208, 1177, 1161, 1126,

1112, 1092, 1068, 1054, 1004, 994, 978, 897, 839, 760, 744, 736, 729, 729, 718, 692, 681, 664, 644, 635, 618, 608, 581, 575, 560, 540, 514 cm^{-1}. MS, *m/z* (%): 324.1 (100, M), 295.1 (41), 275.1 (29), 193.1 (6), 165.1 (14), 162.0 (11), 137.5 (6), 105.0 (5), 77.0 (14). HRMS, (EI) for ($C_{20}H_{11}F_3O^+$): calcd 324.0762, found 324.0761. Anal. Calcd. for $C_{20}H_{11}F_3O$: C, 74.07; H, 3.42. Found: C, 74.24; H, 3.61.

1-(Perfluorophenyl)-3-phenylisobenzofuran (**7**). An argon filled 50 mL two-necked flask equipped with stir bar and a gas condenser was charged with magnesium turnings (535 mg, 22.000 mmol). After three successive vacuum/argon cycles, ether (40 mL) and one grain of iodine were added, and brownish suspension was stirred for 15 min at room temperature. Subsequently 1-bromopentafluorobenzene (2.67 mL, 21.404 mmol) was added dropwise during 15 min. An exothermic reaction was followed by changes of the color of the reaction mixture from original brown, through colorless to final grayish. This suspension was stirred 60 min at room temperature and then the 3-phenylisobenzofuran-1(3*H*)-one (**19**) (3.000 g, 14.269 mmol) was added and stirring continued for 16 h. Subsequently Ac_2O (4 mL) was added dropwise and the reaction mixture was refluxed at the temperature of the oil bath 70 °C for additional 30 min. A dense yellowish precipitate was formed. Then a saturated and degassed aqueous solution of $NaHCO_3$ (15 mL) was added from a syringe and the aqueous phase was carefully removed with a syringe. The precipitate was filtered off on frit, washed with hexane (2 × 10 mL) and thoroughly dried under reduced pressure (600 mTorr, 25 °C). Compound **7** was obtained as a yellow crystalline solid (2.748 g, 7.627 mmol, 53%).

Mp 167.8 - 169.3 °C (dec.). ^{1}H NMR (400 MHz, $CDCl_3$): δ 7.06 - 7.11 (m, 2H), 7.34 - 7.38 (m, 1H), 7.41 - 7.44 (m, 1H), 7.49 - 7.53 (m, 2H), 7.87 - 7.90 (m, 1H), 7.93 - 7.96 (m, 2H). ^{13}C {^{1}H} NMR (100 MHz, $CDCl_3$): δ 106.9 (td, $^1J_{C,F}$ = 16.5 Hz, $^2J_{C,F}$ = 4.0 Hz), 119.4 (t, $J_{C,F}$ = 4.7 Hz), 120.1, 121.2, 125.3, 126.1, 126.2, 127.9, 129.0, 130.0, 130.9, 138.1 (m), 140.5 (m), 143.6 (m), 147.6. ^{19}F NMR (376 MHz, $CDCl_3$): δ -285.67 - -285.53 (m, 2F), -278.87 - -287.76 (m, 1F), -263.83 - -263.75 (m, 2F). IR (KBr): 3092, 3064, 3024, 1685, 1632, 1599, 1521, 1496, 1451, 1421, 1380, 1368, 1323, 1199, 1185, 1166, 1159, 1143, 1130, 1103, 1072, 1033, 1021, 987, 948, 907, 828, 784, 764, 742, 724, 701, 688, 660, 636, 579, 552, 488 cm^{-1}. MS, *m/z* (%): 360.1 (100, M), 340.0 (10), 331.1 (14), 311.0 (21), 293.1 (12), 255.0 (8), 180.0 (5), 165.1 (6). HRMS, (EI) for ($C_{20}H_9OF_5^+$): calcd 360.0574, found 360.0573. Anal. Calcd. for $C_{20}H_9OF_5$: C, 66.67; H, 2.52. Found: C, 66.50; H, 2.52.

General Procedure for Synthesis of Symmetric Fluorinated Derivatives of 1 (GP2).

An argon filled 50 mL two-necked flask equipped with stir bar and a gas condenser was

charged with magnesium turnings (165 mg, 6.800 mmol). After three successive vacuum/argon cycles, THF (15 mL) and one grain of iodine were added, and brownish suspension was stirred for 15 min at room temperature. Subsequently fluorinated bromobenzene (6.700 mmol) was added. An exothermic reaction was followed by changes of the color of the reaction mixture from original brown, through colorless to final grayish. This suspension was stirred 2 h at room temperature and then cooled to -50 °C. A white solid precipitated. Subsequently, methyl 2-formylbenzoate (**20**) (500 mg, 3.046 mmol) was added into vigorously stirred suspension. Cooling was stopped and the reaction mixture was slowly allowed to reach room temperature and then stirred for additional 16 h. The suspension dissolved at ca -5 °C leaving dark red solution, which then slowly changed color to orange and the dense yellowish solid slowly precipitated during subsequent stirring. Then Ac_2O (4 mL) was added dropwise (the suspension dissolved leaving a clear yellow/orange solution) and the reaction mixture was refluxed at the temperature of the oil bath 70 °C for additional 30 min. A dense yellowish precipitate was formed again. Yellow suspension was cooled to room temperature, diluted with ether (100 mL), and washed with a saturated aqueous solution of $NaHCO_3$ (3 × 15 mL). Deep yellow organic phase was dried over $MgSO_4$. Solvents were removed under reduced pressure and column chromatography on silica gel (hexane/ethyl-acetate - 4:1) afforded products as yellow crystalline solids.

1,3-Bis(4-fluorophenyl)isobenzofuran (**8**)[14] was synthesized from 1-bromo-4-fluorobenzene (**13**) (736 μL, 6.700 mmol), magnesium (165 mg, 6.800 mmol), and **20** (500 mg, 3.046 mmol) in THF (15 mL) according to **GP2**. Compound **8** was obtained as a bright yellow crystalline solid (419 mg, 1.368 mmol, 45%).

Mp 138.9 - 139.4 °C. ^{1}H NMR (400 MHz, $CDCl_3$): δ 7.00 - 7.03 (m, 2H), 7.16 - 7.20 (m, 4H), 7.74 - 7.76 (m, 2H), 7.86 - 7.89 (m, 4H). ^{13}C {^{1}H} NMR (100 MHz, $CDCl_3$): δ 116.0 (d, $J_{C,F}$ = 22.0 Hz), 119.8, 121.6, 125.3, 126.4 (d, $J_{C,F}$ = 7.9 Hz), 127.9 (d, $J_{C,F}$ = 3.4 Hz), 142.9, 161.7 (d, $J_{C,F}$ = 247.8 Hz). ^{19}F NMR (376 MHz, $CDCl_3$): δ -238.11 (m, 2F). IR (KBr): 3055, 1628, 1598, 1550, 1514, 1504, 1443, 1410, 1402, 1299, 1291, 1229, 1223, 1201, 1152, 1098, 1092, 1001, 974, 935, 824, 799, 748, 744, 733, 712, 705, 695, 653, 636, 603, 558, 550, 499 cm^{-1}. MS, *m/z* (%): 306.1 (100, M), 277.1 (50), 257.1 (20), 211.1 (5), 183.1 (14), 153.0 (12), 128.5 (7), 95.0 (12), 75.0 (11). HRMS, (EI) for ($C_{20}H_{12}F_2O_2^+$): calcd 306.0856, found 306.0857. Anal. Calcd. for $C_{20}H_{12}F_2O_2$: C, 78.42; H, 3.95. Found: C, 78.35; H, 4.08.

1,3-Bis(3-fluorophenyl)isobenzofuran (**9**) was synthesized from 1-bromo-3-fluorobenzene (**14**) (748 μL, 6.700 mmol), magnesium (165 mg, 6.800 mmol), and **20** (500 mg, 3.046 mmol) in THF (15 mL) according to **GP2**. Compound **9** was obtained as a bright yellow crystalline solid

(637 mg, 2.080 mmol, 68%).

Mp 139.8 - 141.2 °C. ^{1}H NMR (500 MHz, $CDCl_3$): δ 7.00 (m, 2H), 7.04 – 7.09 (m, 2H), 7.44 (m, 2H), 7.60 (m, 2H), 7.70 (m, 2H), 7.78 – 7.83 (m, 2H). ^{13}C {^{1}H} NMR (125 MHz, $CDCl_3$): δ 111.5 (d, $J_{C,F}$ = 23.7 Hz), 113.9 (d, $J_{C,F}$ = 21.5 Hz), 119.9, 120.4 (d, $J_{C,F}$ = 2.8 Hz), 122.7, 125.8, 130.5 (d, $J_{C,F}$ = 8.6 Hz), 133.2 (d, $J_{C,F}$ = 8.6 Hz), 142.9 (d, $J_{C,F}$ = 3.2 Hz), 163.2 (d, $J_{C,F}$ = 245.4 Hz). ^{19}F NMR (470 MHz, $CDCl_3$): δ -108.73 (ddd, $^{1}J_{F,H}$ = 10.3 Hz, $^{2}J_{F,H}$ = 8.4 Hz, $^{3}J_{F,H}$ = 6.0 Hz, 2F). IR (KBr): 3084, 3033, 1625, 1610, 1581, 1541, 1502, 1487, 1464, 1451, 1270, 1261, 1198, 1192, 1171, 1159, 1108, 1067, 998, 995, 879, 869, 856, 850, 830, 778, 774, 750, 743, 684, 562, 527 cm^{-1}. MS, *m/z* (%): 306.1 (100, M), 288.1 (76), 277.1 (21), 257.1 (20), 239.1 (10), 211.1 (11), 183.1 (19), 153.0 (10), 144.0 (7). HRMS, (EI) for ($C_{20}H_{12}F_2O^+$): calcd 306.0856, found 306.0859. Anal. Calcd. for $C_{20}H_{12}F_2O$: C, 78.42; H, 3.95. Found: C, 78.21; H, 3.78.

1,3-Bis(3,5-difluorophenyl)isobenzofuran (**10**) was synthesized from 1-bromo-3,5-difluorobenzene (**15**) (772 µL, 6.700 mmol), magnesium (165 mg, 6.800 mmol), and **20** (500 mg, 3.046 mmol) in THF (15 mL) according to **GP2**. Compound **10** was obtained as a bright yellow crystalline solid (395 mg, 1.153 mmol, 38%).

Mp 197.0 - 198.2 °C. ^{1}H NMR (600 MHz, $CDCl_3$): δ 6.72 - 6.80 (m, 2H), 7.12 - 7.16 (m, 2H), 7.41 - 7.45 (m, 4H), 7.79 - 7.82 (m, 2H). ^{13}C {^{1}H} NMR (150 MHz, $CDCl_3$): δ 102.6 (t, $J_{C,F}$ = 25.7 Hz), 107.4 (m), 119.7, 123.3, 126.6, 133.5 (t, $J_{C,F}$ = 10.5 Hz), 142.4 (t, $J_{C,F}$ = 3.7 Hz), 163.5 (dd, $^{1}J_{C,F}$ = 248.1 Hz, $^{2}J_{C,F}$ = 13.4 Hz). ^{19}F NMR (470 MHz, $CDCl_3$): δ -105.23 (m, 4F). IR (KBr): 3097, 1620, 1590, 1547, 1499, 1475, 1455, 1443, 1406, 1323, 1310, 1261, 1235, 1223, 1192, 1118, 1107, 1003, 986, 863, 854, 840, 828, 820, 744, 729, 678, 653, 645, 533, 521, 508 cm^{-1}. MS, *m/z* (%): 342.1 (100), 313.1 (19), 293.1 (14), 229.0 (13), 201.1 (16), 171.0 (8). HRMS, (EI) for ($C_{20}H_{10}F_4O^+$): calcd 342.0668, found 342.0671. Anal. Calcd. for $C_{20}H_{10}F_4O$: C, 70.18; H, 2.94. Found: C, 69.92; H, 2.83.

1,3-Bis(3,4,5-trifluorophenyl)isobenzofuran (**11**) was synthesized from 5-bromo-1,2,3-trifluorobenzene (**16**) (800 µL, 6.700 mmol), magnesium (165 mg, 6.800 mmol), and **20** (500 mg, 3.046 mmol) in THF (15 mL) according to **GP2**. Compound **11** was obtained as a bright yellow crystalline solid (486 mg, 1.285 mmol, 42%).

Mp 205.8 - 207.4 °C. ^{1}H NMR (500 MHz, $CDCl_3$): δ 7.12 - 7.15 (m, 2H), 7.47 - 7.52 (m, 4H), 7.72 - 7.76 (m, 2H). ^{13}C {^{1}H} NMR (125 MHz, $CDCl_3$): δ 108.7 (m), 119.4, 122.9, 126.7, 126.8 (td, $^{1}J_{C,F}$ = 8.9 Hz, $^{2}J_{C,F}$ = 5.0 Hz), 138.9 (dt, $^{1}J_{C,F}$ = 254.0 Hz, $^{2}J_{C,F}$ = 15.6 Hz), 141.6 (td, $^{1}J_{C,F}$ = 3.2 Hz, $^{2}J_{C,F}$ = 1.0 Hz), 151.8 (ddd, $^{1}J_{C,F}$ = 249.9 Hz, $^{2}J_{C,F}$ = 10.5 Hz, $^{3}J_{C,F}$ = 4.5 Hz). ^{19}F NMR (470 MHz, $CDCl_3$): δ -157.41 (tt, $J_{F,F}$ = 20.4 Hz, $J_{F,H}$ = 6.4 Hz, 2F), -129.53 (m, 4F). IR

(KBr): 3098, 1630, 1618, 1592, 1552, 1518, 1469, 1449, 1434, 1426, 1332, 1278, 1250, 1230, 1191, 1042, 1023, 998, 874, 858, 850, 834, 824, 771, 749, 742, 676, 634, 626, 590, 557, 519 cm^{-1}. MS, *m/z* (%): 378.0 (100, M), 349.0 (20), 342.1 (12), 331.1 (18), 329.0 (17), 311.1 (10), 247.0 (9), 189.0 (11). HRMS, (EI) for ($C_{20}H_8F_6O^+$): calcd 378.0479, found 378.0482. Anal. Calcd. for $C_{20}H_8F_6O$: C, 63.50; H, 2.13. Found: C, 63.28; H, 2.12.

1,3-Bis(perfluorophenyl)isobenzofuran (**12**). An argon filled 25 mL two-necked flask equipped with stir bar and a gas condenser was charged with magnesium turnings (51 mg, 2.100 mmol). After three successive vacuum/argon cycles, ether (5 mL) and one grain of iodine were added, and a brownish suspension was stirred for 15 min at room temperature. Subsequently 1-bromopentafluorobenzene (249 μL, 1.999 mmol) was added dropwise. An exothermic reaction was followed by changes of the color of the reaction mixture from original brown, through colorless to final grayish. This suspension was stirred 20 min at room temperature and then a solution of 3-(perfluorophenyl)isobenzofuran-1(3*H*)-one (**19**) (300 mg, 0.999 mmol) in ether (10 mL) was added dropwise and stirring continued for 4 h. A dense white solid precipitated. Subsequently trifluoroacetic acid (1 mL) was added dropwise and the reaction mixture was stirred for additional 10 min. The reaction mixture was diluted with ether (50 mL), washed with a saturated aqueous solution of $NaHCO_3$ (2 × 30 mL), and dried over $MgSO_4$. Solvent was removed under reduced pressured and column chromatography on silica gel (hexane/ethyl acetate - 3:1) yielded **12** as an yellow crystalline solid (360 mg, 0.800 mmol, 80%).

Mp 124.6 - 125.8 °C (dec.). ^{1}H NMR (500 MHz, $CDCl_3$): δ 7.13 - 7.16 (m, 2H), 7.44 - 7.48 (m, 2H). ^{13}C {^{1}H} NMR (125 MHz, $CDCl_3$): δ 106.2 (td, $^1J_{C,F}$ = 16.3 Hz, $^2J_{C,F}$ = 4.2 Hz), 119.2 (t, $J_{C,F}$ = 4.2 Hz), 125.4, 126.3, 133.7, 138.1 (m), 141.0 (m), 143.8 (m). ^{19}F NMR (376 MHz, $CDCl_3$): δ -263.08 - -263.16 (m, 4F), -276.73 - -276.84 (m, 2F), -284.91 - -285.05 (m, 4F). IR (KBr): 1651, 1557, 1525, 1517, 1497, 1447, 1396, 1379, 1371, 1342, 1316, 1222, 1199, 1168, 1145, 1115, 1106, 1045, 898, 847, 842, 802, 789, 782, 749, 742, 727, 667, 632, 615, 579, 436 cm^{-1}. MS, *m/z* (%): 450.0 (100, M), 431.0 (8), 421.0 (7), 403.0 (42), 383.0 (28), 372.0 (21), 352.0 (10), 334.0 (11), 255.0 (52), 205.0 (10), 186.0 (11), 167.0 (19), 117.0 (12). HRMS, (EI) for ($C_{20}H_4F_{10}O^+$): calcd 450.0102, found 450.0099. Anal. Calcd. for $C_{20}H_4F_{10}O$: C, 53.35; H, 0.90. Found: C, 53.25; H, 1.09.

3-(Perfluorophenyl)isobenzofuran-1(*3H*)-one (**21**). An argon filled 50 mL two-necked flask equipped with stir bar and a gas condenser was charged with magnesium turnings (177 mg, 7.300 mmol). After three successive vacuum/argon cycles, ether (10 mL) and one grain of iodine were added, and brownish suspension was stirred for 15 min at room temperature. Subsequently 1-

bromopentafluorobenzene (873 μL, 7.059 mmol) was added dropwise during 15 min. An exothermic reaction was followed by changes of the color of the reaction mixture from original brown, through colorless to final grayish. This suspension was stirred 60 min at room temperature and then cooled to -40 °C. Then methyl 2-formylbenzoate (**20**) (500 mg, 3.046 mmol) was added and stirring continued for 2 h at 0 °C. A grayish precipitate was formed. Subsequently trifluoroacetic acid (1 mL) was added dropwise and the reaction mixture was stirred for additional 10 min at room temperature. A dense yellowish precipitate was formed. The reaction mixture was diluted with ether (150 mL), washed with a saturated aqueous solution of $NaHCO_3$ (2 × 30 mL), and dried over $MgSO_4$. Solvent was removed under reduced pressured and column chromatography on silica gel (hexane/ethyl acetate - 2:1) afforded **21** as a white crystalline solid (728 mg, 2.425 mmol, 80%).

Mp 114.5 - 115.8 °C (dec.). ^{1}H NMR (400 MHz, $CDCl_3$): δ 6.73 (s, 1H), 7.33 - 7.36 (m, 1H), 7.60 - 7.64 (m, 1H), 7.69 - 7.73 (m, 1H), 7.99 - 8.01 (m, 1H). ^{13}C {^{1}H} NMR (100 MHz, $CDCl_3$): δ 71.9, 110.3, 122.0, 125.7, 126.1, 130.1, 134.7, 139.0 (m), 140.8 (m), 144.2 (m), 146.8, 169.3. ^{19}F NMR (376 MHz, $CDCl_3$): δ -263.06 - -263.14 (m, 2F), -276.71 - -276.82 (m, 1F), -284.89 - -285.03 (m, 2F). IR (KBr): 3088, 3066, 3033, 1803, 1774, 1726, 1655, 1611, 1601, 1524, 1507, 1475, 1468, 1427, 1388, 1349, 1338, 1308, 1286, 1260, 1211, 1191, 1161, 1139, 1127, 1116, 1102, 1052, 1001, 956, 893, 869, 807, 760, 750, 736, 702, 692, 662, 646, 595, 580, 523, 494 cm^{-1}. MS, *m/z* (%): 301.0 (100, M + H). HRMS, (APCI) for ($C_{14}H_5O_2F_5 + H^+$): calcd 301.02825, found 301.02829. Anal. Calcd. for $C_{14}H_5F_5O_2$: C, 56.02; H, 1.68. Found: C, 55.81; H, 1.82.

3 RESULTS

3.1 Synthesis

Both the asymmetrically (**2** - **8**) and symmetrically (**9** - **12**) substituted fluorinated derivatives of **1** were prepared by one-pot reaction[33] shown in Scheme 1. Grignard reagents obtained from **13** - **18** were treated with 3-phenylisobenzofuran-1(3*H*)-one (**19**) and the reaction mixtures were quenched with CF_3COOH[14] or Ac_2O[13] to afford the asymmetric compounds **2** - **8**. The symmetrically substituted derivatives **9** - **12** were synthesized under almost identical reaction conditions, but using methyl 2-formylbenzoate (**20**) instead of **19**. Relatively low yields were attributed mostly to a combination of low stability of some of the fluorinated Grignard reagents and the general instability of the products, which in some cases rapidly decomposed during purification.

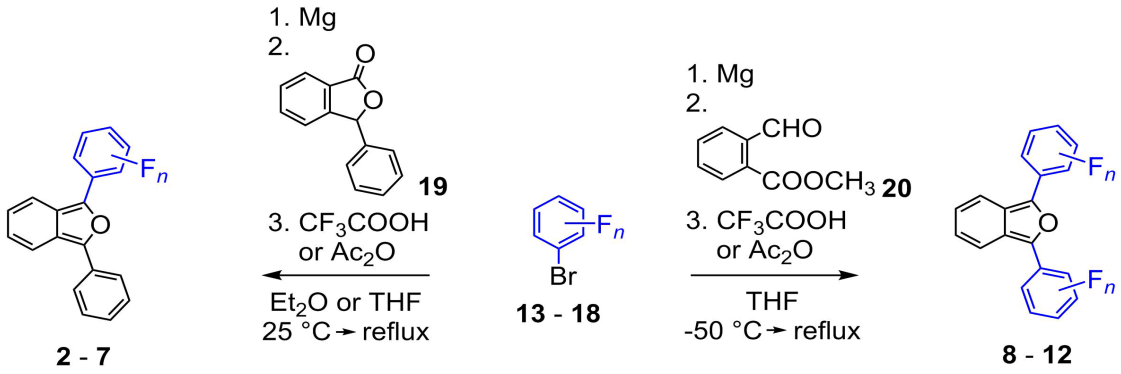

	13	**14**	**15**	**16**	**17**	**18**
Cmpd.	**2** (31%)	**3** (89%)	**4** (60%)	**5** (70%)	**6** (10%)	**7** (53%)
	8 (45%)	**9** (68%)	**10** (38%)	**11** (42%)		**12** (54%)

Scheme 1. One-pot syntheses of asymmetrically (**2** - **8**) and symmetrically (**9** - **12**) substituted fluorinated derivatives of **1**.

A two-step approach was tested on the synthesis of **12**. A low-temperature reaction of **20** with a slight excess of the Grignard reagent derived from **18** afforded **21** in a high yield (Scheme 2). Addition of a second equivalent of the same Grignard reagent resulted in nearly quantitative formation of **12** based on ^{1}H NMR. The low stability of the product caused losses during isolation and purification and reduced the yield to 80%.

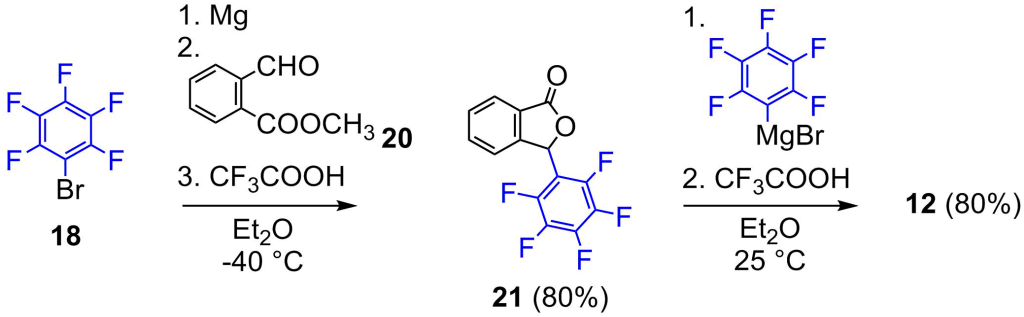

Scheme 2. A two-step synthesis of **12**.

3.2 **Electrochemistry**

The choice of material of the working electrode, Hg, Pt, glassy carbon (GC), or boron doped diamond (BDDE) had negligible effect on the results, suggesting the absence of electrode-assisted (adsorption) effects. The measured currents were linear with substrate concentration and with square root of scan rate, as expected for diffusion-controlled redox processes.

The reduction of compounds **1 – 12** involves several steps (Table 1), suggesting a complicated mechanism. Three reduction patterns have been found. Compounds **2-4, 6, 8-10**, with up to four fluorine atoms in the molecule (except **5**), behave like the parent **1**. Their first reduction steps are reversible and one-electron, and are followed by another one-electron step. The reversibility and formation of a stable radical anion were proven by cyclic voltammetry and in-situ EPR spectroelectrochemistry. The values of all redox potentials vary regularly and additively with the number and position of the fluorine atoms (Table 1).

Compounds **5** and **11** follow a second pattern, where after the first one-electron reduction a two electron process occurs. A third pattern is observed with **7** and **12**, whose molecules contain one or two fully fluorinated phenyl rings, and where an irreversible first reduction step involves two electrons. Only a very weak structureless EPR signal is observed at the first reduction step, suggesting that the initial reduction product is unstable.

In the accessible potential range all compounds **1 - 12** are oxidized similarly in a single irreversible step (Figure 2), therefore only the first anodic peak potentials and currents were considered. From comparison of anodic peak currents with those of the first reduction steps of **2 - 4**, **6**, and **8 – 10** follows that the first oxidation step is a two-electron process.

Although the really correct correlation of experimental data with the quantum chemical calculations is possible only for reversible processes (valid for the first reduction), we tried to correlate the calculations also with the first oxidation step, though it behaves irreversibly. Considering that the first anodic peak potentials were practically constant with increasing scan rate (50-500mV.s^{-1}), it points to the fact, that the overpotential is not significant, the irreversibility (absence of the counter peak) is caused by fast follow-up reaction whereas the primary oxidation potential is close to the reversible one. This interpretation was supported by very good correlation of experimental oxidation potential with the calculated electrochemical oxidation potentials (Fig. S6a in supporting information) as well as with calculated HOMO energies (Fig. S7a).

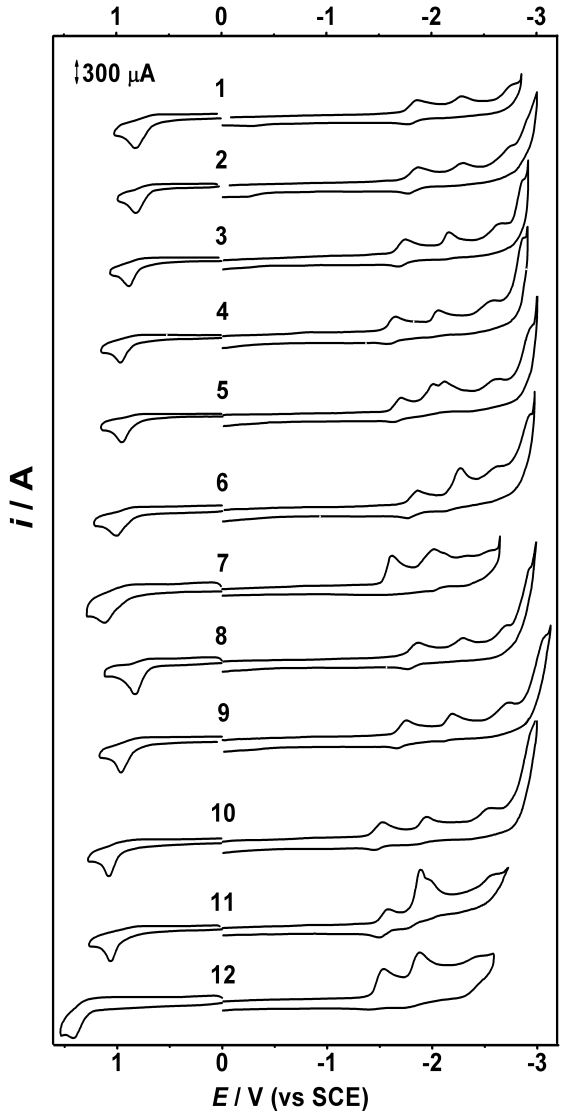

Figure 2. Cyclic voltammograms of **1** - **12** in DMF at 25 °C, glassy carbon electrode, 0.2 V/s, 0.1 M [*n*Bu_4N][PF_6] vs SCE

Table 1: Table of experimental electrochemical data of **1** – **12** (conc. 1mM) on glassy carbon electrode taken from CV at 100 $mV.s^{-1}$ (in V relative to SCE).

	oxidn.	first reduction step			other reduction steps[d]				
Cmpd.	$E_{pa}(1)$[a]	$E_{pc}(1)$	$E_{pa}(1)$[b]	$E^0(1)$[c]	$E_{pc}(2)$	$E_{pc}(3)$	$E_{pc}(4)$	$E_{pc}(5)$	$E_{pc}(6)$
1	0.79	-1.89	-1.81	-1.85	-2.32			-2.81	
2	0.80	-1.90	-1.82	-1.86	-2.32			-2.77	-2.98
3	0.87	-1.81	-1.74	-1.775	-2.23			-2.73	-2.98
4	0.93	-1.72	-1.64	-1.68	-2.15			-2.67	-2.99
5	0.91	-1.75	-1.67	-1.71	-2.05	-2.15		-2.66	-3.00
6	0.99	-1.90	-1.83	-1.865	-2.29			-2.70	-2.98
7	1.12	-1.69	[e]	–	-2.03	-2.11	-2.42	-2.66	
8	0.82	-1.90	-1.82	-1.86	-2.33			-2.77	-3.05
9	0.94	-1.73	-1.65	-1.69	-2.16			-2.68	-2.99
10	1.05	-1.56	-1.49	-1.525	-1.99			-2.60	-2.99
11	1.04	-1.60	-1.51	-1.555	-1.90	-1.99		-2.63	-3.00
12	1.39	-1.59	[e]	–	-1.94	-2.25		-2.53	

[a] E_{pa} are the first anodic peak potentials.

[b] E_{pa} are the counter peak potentials of the first reduction step.

[c] E^0 are the first reduction potentials (reversible) obtained from cyclic voltammetry as $(E_{pc} + E_{pa})/2$

[d] E_{pc} are the cathodic peak potentials. Accuracy (reproducibility and repeatability) is ± ≤10mV.

[e] Different reduction pattern: two-electron step, where anodic counter peak is missing.

3.3 **Calculations**

3.3.1 **Interatomic Distances** (Figure 3 and Table S1). In the neutral compounds **1** - **12**, calculated bond lengths are not significantly affected by fluorine substitution. The length of the C-

O bonds *a* and *e* is 137.0 - 137.6 pm, that of the C=C bonds *b* and *d* 139.2 - 140.1 pm, that of the aromatic C-C bonds *c* 145.1 - 145.4 pm, and that of the exocyclic C-C bonds *f* and *g*, 144.5 - 145.1 pm. In the radical anions of **1** - **12**, the C-O bonds *a* and *e* are noticeably longer (139.8 - 140.3 pm) and the C=C bonds *b* and *d* slightly longer (141.0 - 141.7 pm). In contrast, the length of bond *c* remains almost unchanged (145.2 - 145.9 pm) and the bonds *f* and *g* are □2 pm shorter (142.1 - 143.3 pm). In the radical cations of **1** - **12**, the calculated length of C-O bonds *a* and *e* (136.9 - 137.3 pm) is essentially the same as in the neutrals, but the C=C bonds *b* and *d* are significantly elongated (141.3 - 142.2 pm), and the bond *c* is shortened (143.7 - 143.9 pm). The exocyclic C-C bonds *f* and *g* (142.9 - 143.9 pm) are slightly shorter (144.5 - 145.1 pm).

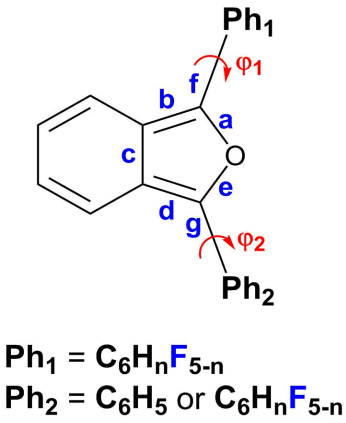

Figure 3. Labels for interatomic distances and torsion angles (see Table S1).

3.3.2 **Torsion angles**. Substitution of hydrogen by fluorine atoms in meta and para position of phenyl rings Ph(1) and Ph(2) (Figure 3) does not affect the calculated torsion angles with the plane of the isobenzofurane moiety, φ_1 and φ_2. Not surprisingly, fluorine atoms in the ortho positions of these phenyl rings increase the torsion angle φ_1 in **6** and **7**, and both φ_1 and φ_2 in **12**.

In the neutral compounds that do not carry fluorine atoms in ortho positions, the angles φ_1 and φ_2 are 18.5 - 23.5°. The radical anions are nearly planar, with torsion angles of 0.4 - 8.1°. In contrast, in cation radicals the torsion angles φ_1 and φ_2 (15.7 - 21.7°) are nearly identical with those observed in the neutral compounds.

The fluorine atoms in the ortho positions of **6**, **7**, and **12** cause the phenyl rings to twist more, to 36.9 - 45.0°. This twist angle is slightly reduced in the radical anions (32.0 - 35.3°) and cations (32.8 - 35.5°).

3.3.3 **Standard Reduction Potentials**. Table 2 compares the values obtained from DFT calculations for the first oxidation and reduction potentials using two different choices of functionals with the averages of the potentials measured on all four electrodes used. The calculations relied on a standard procedure: the one-electron reduction potential reflects Gibbs free energy change upon one-electron oxidation of a solute,

$$E^\circ\,[\mathrm{V}] = -\,\Delta G_{\mathrm{red/ox}} - E^\circ_{\mathrm{abs}}[\mathrm{reference}], \qquad (1)$$

where $\Delta G_{\mathrm{red/ox}}$ (= $G_{\mathrm{red}} - G_{\mathrm{ox}}$) is the free energy difference between the reduced and oxidized state of a solute and E°_{abs}[reference] is the absolute potential of a reference electrode. Since we are not aware of any standard recommendation for the absolute potential of SCE in DMF solution, we estimated the E°_{abs}[SCE(DMF)] from $E^\circ_{\mathrm{abs}}[FeCp_2^{+/0}(DMF)]$ (= 4.97 eV; $FeCp_2^{+/0}$ = ferrocenium/ferrocene redox couple) [34], and $FeCp_2^{+/0}$ to SCE scale conversion of 0.45-0.47 eV - see Table 1 in ref. 35. Similarly, one may adopt the absolute potential of standard hydrogen electrode (SHE) in DMF (= 4.29 eV) with SHE to SCE scale conversion of 0.24 eV (reported for an aqueous solution in ref. 36). Both approaches lead to a similar result for SCE in DMF, with an absolute potential of E°_{abs}[SCE(DMF)] = 4.50-4.53 eV. Herein, we adopted a rounded value of 4.5 eV. The $\Delta G_{\mathrm{red/ox}}$ values were evaluated from:[37]

$$\Delta G_{\mathrm{red/ox}} = \Delta E_{\mathrm{el}} + \Delta G_{\mathrm{solv}} + \Delta(E_{\mathrm{ZPVE}} + pV - RT\ln Q) \qquad (2)$$

where ΔE_{el} (= $E_{\mathrm{el,red}} - E_{\mathrm{el,ox}}$) is the energy difference between the reduced and oxidized structures in vacuum, ΔG_{solv} (= $\Delta G_{\mathrm{gsolv,red}} - \Delta G_{\mathrm{solv,ox}}$) is the difference in their solvation energies, and $\Delta(E_{\mathrm{ZPVE}} + pV - RT\ln Q)$ is the difference in the thermal enthalpic and entropic contributions. As documented in several instances, such methodology is expected to provide relative values of reduction potentials within the accuracy of ca. 50 mV [36]. An excellent relative agreement between the experimental and calculated electrochemical potentials is evidenced in Table 2 and in Figure S6a,b in the Supporting Information. We note in passing that a correlation between the energy of HOMO (LUMO) in a series of compounds **1-12** and their oxidation (reduction) potentials also agrees well and is plotted in Figure S7a,b.

Table 2. Experimental data [a] taken from CV at 100 $mV.s^{-1}$ and calculated reduction potentials for "radical cation – neutral" ($E^{+/0}$) and "neutral – radical anion" ($E^{0/-}$) couples (in V against SCE in DMF at 298 K).

Cmpd.	$E^{+/0}$			$E^{0/-}$		
	Exp.[a] ($E_{p,a}$)	B3LYP[b]	PBE[c]	Exp.[a] (E^0_{red})	B3LYP[b]	PBE[c]
1	0.79	0.58	0.66	-1.85	-1.74	-1.54
2	0.80	0.57	0.63	-1.86	-1.73	-1.54
3	0.87	0.64	0.72	-1.775	-1.65	-1.47
4	0.93	0.72	0.77	-1.68	-1.54	-1.38
5	0.91	0.73	0.76	-1.71	-1.53	-1.39
6	0.99	0.73	0.78	-1.865	-1.79	-1.61
7	1.12	0.87	0.89	-1.69[e]	-1.58	-1.43
8	0.82	0.56	0.60	-1.86	-1.73	-1.56
9	0.94	0.71	0.77	-1.69	-1.51	-1.35
10	1.05	0.87	0.89	-1.525	-1.36	-1.23
11	1.04	0.88	0.85	-1.555	-1.31	-1.21
12	1.39	1.16	1.10	-1.59[e]	-1.37	-1.26
R^{2} [d]		0.965	0.956		0.962	0.962

[a] Experimental values for oxidation are anodic peak potentials using GC electrode (data from BDDE and Pt electrodes are very close to those of GC), the data for reduction are the first reversible potentials E^0 obtained from cyclic voltammetry on GC as $(E_{pc} + E_{pa})/2$. [b] RI-B3LYP-D3/def2-TZVPD. [c] RI-PBE-D3/def2-TZVPD. [d] R is the regression coefficient. [e] Cathodic peak potentials due to absence of anodic counter peak and thus different reduction pattern: two-electron irreversible step.

4 DISCUSSION

4.1 **Synthesis.** Preparation of all 11 fluorinated DPIBF derivatives was a straightforward process utilizing previously developed reaction conditions[13,14] and does not call for much comment. Two different quenching procedures were tested, using either CF_3COOH or Ac_2O, and produced nearly identical isolated yields. Probably the most noticeable difference was observed immediately after the addition of these reagents: CF_3COOH usually caused the crude reaction mixture to turn black, while it turned deep yellow when Ac_2O was used. The difficult part was the isolation and purification. Although the bright to deep yellow solid products can be stored under an argon atmosphere in a freezer for several months without noticeable decomposition, their solution stability is poor. They require strictly oxygen-free solvent and even then some of them decompose within a few hours. ^{1}H NMR revealed that **1** and **2** are the most stable in $CDCl_3$ solution and did not show any signs of decomposition even after several days in the dark at room temperature.

4.2 **Molecular Geometry**. Single-crystal X-ray diffraction structures reported for the two crystal forms of neutral **1**[7] yield essentially identical molecular geometries, in good agreement with the results shown in Table S1, and an effort to determine the geometries of the neutral species **2** - **12** is underway. They will presumably all be very similar except possibly for the phenyl twist angles. As explained in the introduction, the main interest is in determining crystal packing.

Geometries of the radical ions are much harder to access experimentally, and at this time, only the calculated values listed in Table S1 are available. The bond lengths differ from those in the neutral species in a way that is easily understood by consideration of the distribution of nodal planes in the highest occupied (HOMO) and lowest unoccupied (LUMO) molecular orbitals of isobenzofuran, which is the same in all twelve compounds (Figure S1) and is illustrated for the parent compound **1** in Figure 4. Approximate positions of the nodal planes can be deduced easily from a consideration of the MOs of the [9]annulenide anion perimeter of isobenzofuran. The two degenerate HOMOs of this perimeter have two nodal planes perpendicular to the molecular plane, with nodal points along the perimeter 9/4 of a bond length apart, and the two LUMOs have three, with nodal points 3/2 bond lengths apart. When an oxygen atom replaces one of the carbons to yield oxonine, the energies of the MOs that have a node going through the oxygen atom will not respond to its high electronegativity in the first approximation, whereas those that do not will be stabilized. Therefore, the HOMO will have a node going through the oxygen and the LUMO will not. When a cross-link is introduced to convert oxonine to isobenzofuran, the HOMO will be destabilized and LUMO will be stabilized, and their status as the frontier orbitals reinforced. Once the locations of the nodal points on the isobenzofuran perimeter have been established, the relative amplitudes of the MOs at various perimeter atoms follow - the closer the atom is to a nodal plane, the smaller the amplitude.

Removal of an electron from HOMO will halve its bonding contribution between atoms that are not separated by a node and halve its antibonding contribution between atom that are, and bond lengths will respond correspondingly. Addition of an electron to the LUMO will similarly introduce additional bonding between atoms that are not separated by a node and antibonding between atoms that are, and bond lengths will respond. The magnitude of the effect will reflect the amplitude of the MO on the atoms in question. Thus, oxidation is expected to extend the *b* and *d* bonds and shorten *f*, *g*, and *c* bonds, whereas reduction is expected to extend the *a* and *e* bonds and shorten the *f* and *g* bonds, exactly as is observed in Table S1.

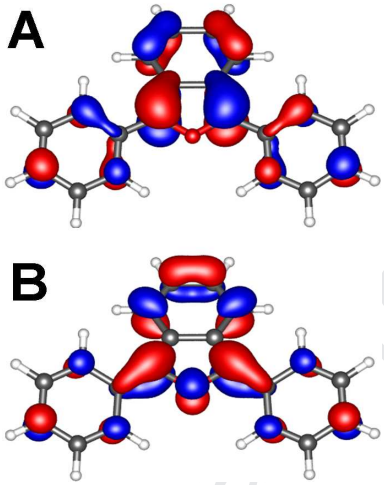

Figure 4. Frontier molecular orbitals of **1**: (a) HOMO and (b) LUMO.

4.3 **Redox Potentials.** The relative values of the first oxidation and first reduction potentials of compounds **1 - 12** are well reproduced by DFT calculations (Table 2), with high regression coefficients. However, a large shift of the regression line is also observed, suggesting that our theoretical model does not fit the measured electrochemical potentials absolutely. The shift from the experimental values in average corresponds to –0.24 V and +0.19 V for the B3LYP method for "radical cation – neutral" and "neutral – radical anion" reduction couples, or –0.21 V and +0.34 V for the PBE method, respectively. The shift is not particularly surprising as the scaling of the experimental values to the absolute potential depends on the experimental setup, calibration of electrode used, surface potential, etc.

It is useful to obtain qualitative intuitive insight as well, since it is easily transferred to related compounds. This is obtained by considering the two phenyl substituents as a perturbation of the electronic structure of isobenzofuran and using standard notions for the description of

substituent effects. By extending the π system, the phenyl groups act as substituents with both resonance and inductive effects, increasing the energy of the HOMO and lowering that of the LUMO of isobenzofuran, to a degree that depends on the phenyl twist angle. The fluorine atoms on the phenyl rings modulate their inductive and resonance effects. The latter can occur in two ways, directly when the fluorine substituents are in ortho or para positions, and indirectly via their steric effects on the phenyl twist angles when they are in ortho positions. Comparison of results for **1 - 12** shows that every fluorine atom in the meta position on a phenyl substituent makes the first reduction easier by ~80 mV, and this can be attributed to its inductive effect. In contrast, para and ortho fluorine atoms on the phenyl substituents have practically no effect on the first reduction potentials. In the case of para substitution, this can be understood as a result of compensation of the now weaker electron-withdrawing inductive effect of the fluorine by its weak electron-donating resonance effect. For ortho fluoro substitution the inductive effect would then be expected to dominate over the resonance effect, facilitating the first reduction, but it is apparently just compensated by the sterically induced increase in the phenyl twist angle that makes the reduction harder.

The results for anodic potentials can be understood similarly. The inductive effect of every meta fluorine makes the oxidation harder by 50-60 mV, which is consistent with its effect on reduction, and the negligible influence of a para fluorine on the oxidation potential can be understood in the same way as in the case of the reduction potential. Now, however, the inductive and the sterically induced reduction of the resonance effect due to the two ortho fluorine substituents at each phenyl do not compensate each other but add, making the oxidation more difficult by ~180 mV.

These simple considerations may be intuitively satisfying but are strictly qualitative. A more detailed comparison of the magnitudes of substituent effects on the oxidation and reduction potentials would require a knowledge of the relative amplitudes of the HOMO and the LUMO in the position of attachment of the perturbing phenyl substituent and hence a computation. For such quantitative work we consider it preferable to perform a DFT calculation as discussed above.

5 SUMMARY

A series of fluorinated 1,3-diphenylisobenzofurans was synthesized and characterized by

standard electrochemical methods. For most of the compounds, the first reduction step is reversible and the formation of an intermediate radical anion was proved by cyclic voltammetry and EPR spectroelectrochemistry. The redox potentials obtained showed significant variation and will be useful in studies of singlet fission. The observed regularities were interpreted qualitatively by consideration of substituent effects and quantitatively by comparison with DFT calculations. The bond length changes expected upon one-electron oxidation or reduction were computed and rationalized.

Four members of the series with the highest numbers of fluorine atoms undergo reduction by a more complicated mechanism that has not been investigated further.

ASSOCIATED CONTENT

Supporting Information. Copies of ^{1}H, ^{13}C NMR spectra of all new compounds, ORTEP view of a single molecule and packing in **21**, calculated geometries of **1** - **12** and their radical cations and anions, correlation between the experimental oxidation (reduction) potentials of compounds **1-12,** their calculated energies HOMO (LUMO) and calculated electrochemical potentials, respectively.

ACKNOWLEDGEMENT

Work in Prague was supported by the grant GAČR 19-22806S, institutional supports of the J. Heyrovský Institute of Physical Chemistry (RVO 61388955), and Institute of Organic Chemistry and Biochemistry (RVO: 61388963). We are grateful to Dr. Ivana Císařová for performing a single-crystal X-ray analysis of compound **21**. Work in the USA was supported by the U.S. DoE BES, Division of Chemical Sciences, Biosciences, and Geosciences (DE-SC0007004).

REFERENCES

1. M. B. Smith, J. Michl, Singlet Fission, Chem. Rev. 110 (2010) 6891.

2. M. B. Smith, J. Michl, Recent Advances in Singlet Fission, Ann. Rev. Phys. Chem. 64 (2013) 361.

3. M. C. Hanna, A. J. Nozik, Solar Conversion Efficiency of Photovoltaic and Photoelectrolysis Cells with Carrier Multiplication Absorbers, J. App. Phys. 100 (2006) 074510.

4. W. Shockley, H. J. Queisser, Detailed Balance Limit of Efficiency of p-n Junction Solar Cells,

J. App. Phys. 32 (1961) 510.

5. I. Paci, J. C. Johnson, X. Chen, G. Rana, D. Popović, D. E. David, A. J. Nozik, M. A. Ratner, J. Michl, Singlet Fission for Dye-Sensitized Solar Cells: Can a Suitable Sensitizer Be Found? J. Am. Chem. Soc. 128 (2006) 16546.

6. J. C. Johnson, A. J. Nozik, J. Michl, High Triplet Yield from Singlet Fission in a Thin Film of 1,3-Diphenylisobenzofuran, J. Am. Chem. Soc. 132 (2010) 16302.

7. J. Ryerson, J. N. Schrauben, A. J. Ferguson, S. C. Sahoo, P. Naumov, Z. Havlas, J. Michl, A. J. Nozik, J. C. Johnson, Two Thin Film Polymorphs of the Singlet Fission Compound 1,3-Diphenylisobenzofuran, J. Phys. Chem. C. 118 (2014) 12121.

8. Z. Havlas, J. Michl, Guidance for Mutual Disposition of Chromophores for Singlet Fission, Isr. J. Chem. 56 (2016) 96.

9. E. A. Buchanan, J. Michl, Packing Guidelines for Optimizing Singlet Fission Matrix Elements in Non-Covalent Dimers, J. Am. Chem. Soc. 139 (2017) 15572.

10. E. A. Buchanan, Z. Havlas, J. Michl, Singlet Fission: Optimization of Chromophore Dimer Geometry, in: J. R. Sabin, E. J. Brändas (Eds.), Eds.Advances in Quantum Chemistry: Ratner Volume, Vol. 75, Elsevier, Cambridge, MA, 2017, p. 175.

11. R. J. Dillon, G. B. Piland, C. J. Bardeen, Different Rates of Singlet Fission in Monoclinic versus Orthorhombic Crystal Forms of Diphenylhexatriene, J. Am. Chem. Soc. 135 (2013) 17278.

12. D. H. Arias, J. L. Ryerson, J. D. Cook, N. H. Damrauer, J. C. Johnson, Polymorphism Influences Singlet Fission Rates in Tetracene Thin Films, Chem. Sci. 7.2 (2016) 1185.

13. P. I. Dron, J. Michl, J. C. Justin, Singlet Fission and Excimer Formation in Disordered Solids of Alkyl-Substituted 1, 3-Diphenylisobenzofurans, J. Phys. Chem. A 121 (2017) 8596.

14. Ch. Dai, P. Nguyen, T. B. Marder, A. J. Scott, W. Cleggc, Ch. Viney, Control of single crystal structure and liquid crystal phase behaviour via arene-perfluoroarene interactions, Chem. Commun. 24 (1999) 2493.

15. M. L. Renak, G. P. Bartholomew, S. Wang, P. J. Ricatto, R. J. Lachicotte, G. C. Bazan, Fluorinated Distyrylbenzene Chromophores: Effect of Fluorine Regiochemistry on Molecular Properties and Solid State Organization, J. Am. Chem. Soc.121 (1999) 7787.

16. J. C. Collings, J. M. Burke, P. S. Smith, A. S., Batsanov, J. A. K. Howard, T. B. Marder, The synthesis and crystal structures of halogenated tolans p-X-C6H4-C C-C6F5 and p-X-C6F4-C C-C6H5 (X = F, Cl, Br, I), Org. Biomol. Chem. 2 (2004) 3172.

17. A. Liška, P. Vojtíšek, A. J. Fry, J. Ludvík, Electrochemical and Quantum Chemical Investigation of Tetranitrocalix[4]arenes: Molecules with Multiple Redox Centers, J. Org. Chem. 78 (2013) 10651.

18. R. Ahlrichs, M. Bar, M. Haser, H. Horn, C. Kolmel, Electronic Structure Calculations on Workstation Computers: The Program System Turbomole, Chem. Phys. Lett. 162 (1989) 165.

19. K. Eichkorn, O. Treutler, H. Öhm, M. Häser, R. Ahlrichs, Auxiliary Basis Sets to Approximate

Coulomb Potentials, Chem. Phys. Lett. 240 (1995) 283.

20. J. P. Perdew, Density-Functional Approximation for the Correlation Energy of the Inhomogeneous Electron Gas, Phys. Rev. B 33 (1986) 8822.

21. A. D. Becke, Density-Functional Exchange-Energy Approximation With Correct Asymptotic Behavior, Phys. Rev. A 38 (1988) 3098.

22. S. Grimme, J. Antony, S. Ehrlich, H. Krieg, A Consistent and Accurate ab initio Parametrization of Density Functional Dispersion Correction (DFT-D) for the 94 Elements H-Pu, J. Chem. Phys. 132 (2010) 154104.

23. F. Weigend, R. Ahlrichs, Balanced Basis Sets of Split Valence, Triple Zeta Valence and Quadruple Zeta Valence Quality for H to Rn: Design and Assessment of Accuracy, Phys. Chem. Chem. Phys. 7 (2005) 3297.

24. A. Klamt, G. Schuurmann, COSMO: A New Approach to Dielectric Screening in Solvents With Explicit Expressions for the Screening Energy and its Gradient, J. Chem. Soc., Perkin Trans. (1993) 799.

25. A. D. Becke, Density Functional Thermochemistry. III. The Role of Exact Exchange, J. Chem. Phys. 98 (1993) 5648.

26. D. Rappoport, F. Furche, Property-Optimized Gaussian Basis Sets for Molecular Response Calculations, J. Chem. Phys. 133 (2010) 134105.

27. J. P. Perdew, K. Burke, M. Ernzerhof, Fluid Vesicles in Shear Flow, Phys. Rev. Lett. 77 (1996) 3865.

28. COSMOtherm, C3.0, release 1701, COSMOlogic GmbH & Co KG, http://www.cosmologic.de.

29. A. Klamt, Conductor-like Screening Model for Real Solvents: A New Approach to the Quantitative Calculation of Solvation Phenomena, J. Phys. Chem. 99 (1995) 2224.

30. S. Grimme, Supramolecular Binding Thermodynamics by Dispersion Corrected Density Functional Theory, Chem. Eur. J. 18 (2012) 9955.

31. G. M. Sheldrick, SHELXT - Integrated Space-Group and Crystal-Structure Determination, Acta Cryst. A71 (2015) 3.

32. G. M. Sheldrick, Crystal Structure Refinement With SHELXL, Acta Cryst. C71 (2015) 3.

33. T. Hamura, R. Nakayama, A One-pot Preparation of 1,3-Diarylisobenzofuran, Chem. Lett. 42 (2013) 1013.

34. P. P. Romańczyk, G. Rotko, S. S. Kurek, The Redox Potential of the Phenyl Radical/Anion Couple and the Effect Thereon of the Lithium Cation: A Computational Study, Electrochem. Commun. 48 (2014) 21.

35. N. G. Connelly, W. E. Geiger, Chemical Redox Agents for Organometallic Chemistry, Chem. Rev. 96 (1996) 877.

36. A. V. Marenich, J. Ho, M. L. Coote, C. J. Cramer and D. G. Truhlar Computational electrochemistry: prediction of liquid-phase reduction potentials. Phys. Chem. Chem. Phys. 16 (2014) 15068.

37. Several relevant conformers/rotamers for each of the oxidized and reduced structure were taken into account. The reduction potential $E°$ is calculated as the difference between the lowest-lying conformers as predicted by the free energy calculations.